J Solid State Electrochem (2005) 9: 816–822
DOI 10.1007/s10008-005-0008-8

ORIGINAL PAPER

Laisheng Sun · Diep Vu Ca · James A. Cox

Electrocatalysis of the hydrogen evolution reaction by nanocomposites of poly(amidoamine)-encapsulated platinum nanoparticles and phosphotungstic acid

Received: 24 March 2005 / Revised: 21 April 2005 / Accepted: 9 May 2005 / Published online: 13 July 2005

Abstract Poly(amidoamine) dendrimer (Generation-4) encapsulated platinum nanoparticles (PtNP-PAMAM) were prepared and used to fabricate nanocomposites with Keggin-type phosphotungstic acid ($PW_{12}O_{40}^{3-}$) using a layer by layer electrostatic assembly technique. Indium tin oxide (ITO) electrodes, which were first modified with a monolayer of 3-aminopropyl triethoxysilane (3-APTES), were used as substrates for assembly of the $PW_{12}O_{40}^{3-}$ monolayer. Nanocomposites were then fabricated by depositing PtNP-PAMAM on the monolayer of $PW_{12}O_{40}^{3-}$. The amount of PtNP-PAMAM deposited was controlled by using different concentrations of PtNP-PAMAM diluted in 0.1 M H_2SO_4 solution. The hydrogen evolution reaction (HER) was used to test electrocatalytic activities of these nanocomposite modified electrodes. Modification of ITO|3-APTES with $PW_{12}O_{40}^{3-}$ |PtNP-PAMAM showed significantly higher electrocatalytic activities toward the HER than electrodes modified with either $PW_{12}O_{40}^{3-}$ or PtNP-PAMAM alone. The electrocatalytic activities were found to depend on the composition of PtNP-PAMAM and $PW_{12}O_{40}^{3-}$ on electrode surfaces, which was attributed to an interaction between these species. Heat treatment of ITO|3-APTES|$PW_{12}O_{40}^{3-}$ |PtNP-PAMAM electrodes at 200 °C produced significantly higher electrocatalytic activities, which supported the suggestion of an interaction.

Keywords Nanoparticles · Platinum · Polyoxometalates · PAMAM · Dendrimers · Electrocatalysis

Presented at the 4th Baltic conference on Electrochemistry, Griefswald, March 13.–16., 2005.

L. Sun · D. V. Ca · J. A. Cox (✉)
Department of Chemistry and Biochemistry,
Miami University Nanotechnology Center,
Miami University, Oxford, OH, 45056 USA
E-mail: coxja@muohio.edu
Tel.: +1-513-5292493
Fax: +1-513-5295715

Introduction

Nanoparticle-based composite films, particularly those with metal centers, on electrode surfaces have attracted a wide scope of investigations due to their potential applications in various fields such as molecular electronics, photonics, electrocatalysis, corrosion protection, and chemical sensors [1]. Attractive features of metal nanoparticles include physical and chemical properties that differ from the corresponding bulk materials due to the quantum size effect [2] and their unique properties in catalysis, including electrocatalysis [3]. For example, platinum nanoparticles (PtNPs), which have potentially important catalytic applications in various industrial fields, have been used as deposits on electrode surfaces to make electrocatalysts for various reactions, such as the reduction of oxygen [4–6], the oxidation of methanol [7], the oxidation of arsenite [8], and the hydrogen evolution reaction [9].

The electrocatalytic activities of PtNPs have been found to be significantly enhanced when supported by redox metal oxides, such as tungsten oxide WO_3 [10, 11]. This enhancement was attributed to a synergistic effect between platinum and WO_3 that resulted in an increase in the amount of active sites on the electrocatalyst surfaces [10]. This proposed synergism is consistent with the report by Kulesza et al. [12] that small quantities of Pt in phosphotungstic acid (PTA), a compound with properties similar to those of WO_3, markedly increased the catalytic efficiency of these polyoxometalates, a finding supported by recent reports [13, 14]. Polyoxometalates are important electrochemical catalysts, whether used alone or as components of composites. They are a distinctive class of nm-sized inorganic metal-oxygen cluster compounds, which can undergo reversible, stepwise multi-electron transfer reactions [15]. A Pt–Co alloy supported on carbon was found to be electroactivated by $SiW_{12}O_{40}^{4-}$, as demonstrated by the fact that the electrocatalytic activity toward the hydrogen evolution reaction (HER) was significantly enhanced [14].

Electrocatalysts fabricated from oxoruthenium-stabilized PtNPs using $PW_{12}O_{40}^{3-}$ as linkers showed enhanced electrocatalytic activities for the electrochemical oxidation of methanol in acidic solutions [16]. The electrocatalytic enhancement was considered to be possibly due to a synergistic effect between Pt–Ru and $PW_{12}O_{40}^{3-}$ [16]. This synergistic effect might be related to changes in surface adsorption properties of platinum. The presence of $PW_{12}O_{40}^{3-}$ on a platinized platinum electrode was reported to affect the adsorption of hydrogen and oxygen on a platinum surface [17].

Various methods have been developed to prepare PtNPs. Monolayer-protected PtNPs, such as alkanethiol-protected PtNPs [18] and recently reported polyoxometalate-protected PtNPs [4], have been used to prepare nanoparticles with diameters less than 10 nm. Electrodeposition has also been used to deposit PtNPs on electrode surfaces; here, the particle sizes are possibly larger than 10 nm and have wide particle size distribution [19, 20]. In recent years, well-defined, almost monodisperse PtNPs have been synthesized using poly(amidoamine), PAMAM, dendrimers as a template [21–23]. In general, PAMAM dendrimers are of interest as templates to prepare metal nanoparticles because they yield nanoparticles with quite uniform composition and structure [24–26]. Metal ions and complexes thereof can be coordinated with interior amine groups. Subsequent chemical reduction produces the corresponding nanoparticles. These encapsulated metal nanoparticles are well defined and nearly monodisperse in sizes ranging from less than 1 nm to 4–5 nm depending on the generation of dendrimer used [26]. More importantly, these nanoparticles are confined to the interior, primarily by steric effects, and they are accessible to reactants in catalytic reactions.

The restriction of NPs to the dendrimer interior also is facilitated by using formulations with terminal hydroxyl groups rather than amines. For example, PAMAM-encapsulated PtNPs (PtNP-PAMAM) that were prepared with G4-PAMAM with terminal hydroxyl groups as a template were almost monodisperse; the diameters were 1.6 ± 0.2 nm [21–23]. Results of the electrocatalytic oxygen reduction on electrodes modified with PtNP-PAMAM modified electrodes showed that the surface of these PtNPs was accessible to oxygen and was able to exchange electrons with the underlying electrode surfaces [21].

Various PAMAM dendrimers have been incorporated into nanocomposites fabricated by the layer-by-layer (LBL) electrostatic assembly technique [27]. Without encapsulated metal nanoparticles, they served as spacers in multilayered assemblies with polyoxometalates (Dawson-type, $P_2W_{18}O_{62}^{-6}$, and Keggin-type, $PMo_{12}O_{40}^{3-}$) or dirhodium-substituted polyoxometalates for electrocatalytic applications [27, 28]. Uniform multilayers containing PAMAM-encapsulated gold nanoparticles also were fabricated using poly(styrene sulfonate) as the oppositely charged polyelectrolyte [29].

The use of hydroxyl-terminated PAMAM, which decreases the number of protonated amine sites relative to the conventional (amine-terminated) dendrimer, does not compromise the ability to fabricate LBL assemblies containing the dendrimer. With high generation numbers (generation-4 PAMAM was used in the present study) interior amine sites, when protonated, provide the charge for electrostatic adsorption to various substrates, and hydrogen bonding can contribute to the process [30, 31]. For example, hydroxyl-terminated PAMAM was strongly adsorbed on mica. It was attributed to the electrostatic attraction between the positively charged PAMAM dendrimer and the negatively charged mica surface as well as hydrogen bonds formed between PAMAM functional groups and the mica surface [31].

In this paper, the LBL electrostatic assembly technique was used to fabricate nanocomposites of Keggin-type PTA ($PW_{12}O_{40}^{3-}$) and poly(amidoamine) dendrimer-encapsulated Pt nanoparticles (PtNP-PAMAM) on electrode surfaces. Generation-4 PAMAM with terminal hydroxyl groups was used. The aims were to test the electrocatalytic activity of PtNP-PAMAM toward the HER and to investigate the effect of the $PW_{12}O_{40}^{3-}$ on the electrocatalytic activities of PtNP-PAMAM. An important objective was to achieve a controlled monolayer-level composite of these components.

Experimental

Materials

Unless otherwise stated, all chemicals were ACS reagent grade from Aldrich Chemical Company (Milwaukee, WI, USA) and used as received. Generation-4 PAMAM with hydroxyl surface groups was purchased as a 10% (weight) solution in methanol. Glass slides coated with indium doped tin oxide (ITO) were obtained from Delta Technologies Limited (Stillwater, MN, USA). Solutions were prepared with the house-distilled water that was further purified with Barnstead NANOpure II system (Boston, MA, USA).

Preparation of PAMAM dendrimer encapsulated Pt nanoparticles

The preparation of PtNP-PAMAM followed a procedure that was previously reported [8]. Briefly, 5 mM PAMAM aqueous solution was prepared from an air-dried aliquot of 10% (weight) PAMAM in methanol. An aliquot (0.25 ml) of the 5 mM PAMAM was then mixed with 25 ml of a vigorously stirred 2 mM K_2PtCl_4 aqueous solution. The mole ratio of Pt^{II} to PAMAM in the mixed solution was 40:1. The mixture was continuously stirred for 4 days to ensure the complete complexation of $PtCl_4^{2-}$ with the interior amine groups of PAMAM. Then, 0.5 ml of 0.5 M $NaBH_4$ solution was quickly added to this mixture, and it was stirred for another 20 min to reduce Pt^{II} to Pt^0. The PtNP-PAMAM solution was used without further treatment.

Fabrication of nanocomposites on electrode surfaces

Before fabrication of nanocomposites, ITO slides were first modified by formation of a monolayer of 3-aminopropyltriethoxysilane (3-APTES) to make the electrode surfaces positively charged in acidic solutions. This modification was carried out by immersing ITO slides in 0.06 M 3-APTES in dry methanol solution overnight. The 3-APTES-modified ITO slides were then rinsed with dry methanol and dried with N_2 gas. A monolayer of $PW_{12}O_{40}^{3-}$ was electrostatically assembled on this surface by immersion in 5 mM $PW_{12}O_{40}^{3-}$ in 0.1 M H_2SO_4 for 1 h. The resulting electrode was rinsed with water and dried with N_2 gas.

Next, PtNP-PAMAM was assembled on the ITO|3-APTES|$PW_{12}O_{40}^{3-}$ electrode by immersion in PtNP-PAMAM solution. The PtNP-PAMAM solution, which was prepared as described above, was diluted in 0.1 M H_2SO_4 prior to assembly of this layer. The use of the acidic solution not only protonated the amine sites of the dendrimer but also prevented decomposition of the polyoxometalate during the fabrication. The amount of PtNP-PAMAM deposited on the monolayer of $PW_{12}O_{40}^{3-}$ was controlled by using different concentrations of the PtNP-PAMAM in 0.1 M H_2SO_4 solution. After immersion for an hour, the electrodes were rinsed with water and dried with N_2 gas.

Films of PtNP-PAMAM and $PW_{12}O_{40}^{3-}$ were also assembled on glassy carbon electrodes with areas of 0.07 cm^2. Prior to each experiment, the glassy carbon was first polished successively with 1.0 and 0.3 μm alpha alumina slurries on cloth and sonicated in water. Because $PW_{12}O_{40}^{3-}$ strongly adsorbs to glassy carbon [32], it was not necessary to modify this electrode material with a cationic layer prior to assembly of this polyanion. The assembly of PtNP-PAMAM followed the same procedure as that for ITO surfaces.

Electrochemical measurements

Electrochemical measurements were carried out in a conventional three-electrode cell using a CH Instruments (Austin, TX, USA) Model 750 instrument. The area of modified ITO electrodes was 1.0 cm^2. A Pt wire was used as the counter electrode, and Ag|AgCl was the reference electrode. The supporting electrolyte was 0.5 M H_2SO_4. Prior to electrochemical measurements, the electrolyte solution was deaerated with N_2; the solution was kept under N_2 during the measurements.

Results and discussion

Prior to deposition of PtNP-PAMAM, cyclic voltammetry of ITO|3-APTES|$PW_{12}O_{40}^{3-}$ in 0.5 M H_2SO_4 was performed (Fig. 1). Four sets of peaks were observed in the potential range of 0.4 to −0.7 V; the formal potentials were −0.045, −0.273, −0.373, and −0.632 V. The

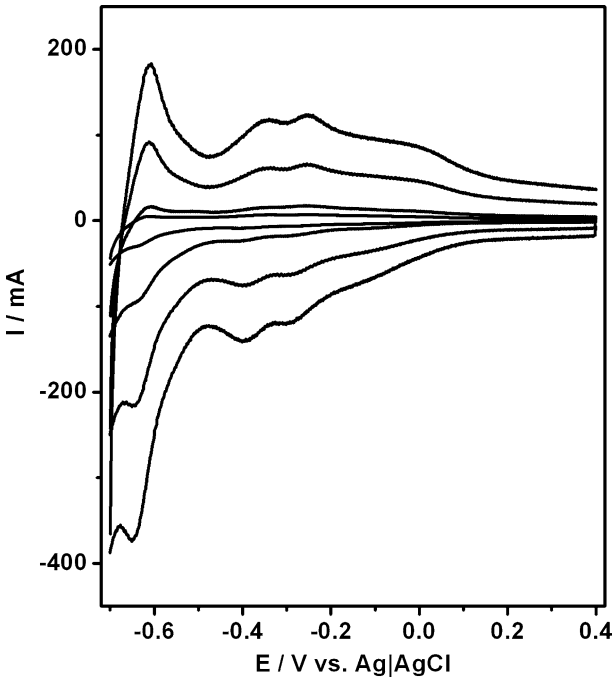

Fig. 1 Cyclic voltammetry of an ITO|3-APTES|$PW_{12}O_{40}^{3-}$ electrode in 0.5 M H_2SO_4 at different scan rates. From the inner to the outer envelop, the scan rates were 0.050, 0.10, 0.50 and 1.0 V s^{-1}

first and the second processes had differences between the anodic and cathodic peak potentials, Δ E_p, of 54 mV and 49 mV, respectively. They presumably correspond to the reversible one-electron redox processes reported for $PW_{12}O_{40}^{3-}$ in 1 M $HClO_4$ aqueous solution [15]. However, the third and the fourth processes, which had respective Δ E_p values of 53 mV and 32 mV, were different from the reported behavior of $PW_{12}O_{40}^{3-}$. In solution, only a third reduction peak was observed before −0.7 V, which was attributed to a reversible two-electron reduction process [15]. This difference possibly resulted from the electrostatic interaction between $PW_{12}O_{40}^{3-}$ and 3-APTES. From the integrated charge of the first cathodic peak in Fig. 1, the surface coverage of $PW_{12}O_{40}^{3-}$ was estimated as 7.3×10^{-11} mol cm^{-2}. Assuming surface behavior (a symmetrical peak), the charge between the onset of the reduction and the peak was measured and doubled to minimize contribution from the second cathodic process. This value was slightly larger than that of $PM_{12}O_{40}^{3-}$ bound to a 4-aminothiolphenol modified Au electrode [27]. The surface of ITO is perhaps rougher than that of gold. In that this value is comparable to the reported coverage of a 3-APTES on ITO surfaces, 5×10^{-11} mol cm^{-2} [33], it is concluded that a monolayer of $PW_{12}O_{40}^{3-}$ was deposited on ITO|3-APTES.

PtNP-PAMAM was then deposited onto the ITO|3-APTES|$PW_{12}O_{40}^{3-}$ from a 0.1 M H_2SO_4 solution, as described in the Experimental section. The intent of this step was to have Pt-PAMAM bind to $PW_{12}O_{40}^{3-}$ exclusively; however, possibility of hydrogen bonding between the terminal hydroxyl groups of the PAMAM

and 3-APTES was not discounted. The concern was the possibility of displacement of some $PW_{12}O_{40}^{3-}$ from the 3-APTES monolayer if that process occurred. In order to address this question, PAMAM without encapsulated PtNPs deposited on the $PW_{12}O_{40}^{3-}$ monolayer using the same assembly procedure as that described in the Experimental section except the PAMAM concentration was 4 μM, a value comparable to that of the dendrimer in the PtNP-PAMAM solution. Figure 2 shows the voltammetry of $PW_{12}O_{40}^{3-}$ before and after PAMAM was deposited. After the deposition of PAMAM, the voltammetric current for $PW_{12}O_{40}^{3-}$ did not change significantly, suggesting that PAMAM was deposited on the $PW_{12}O_{40}^{3-}$ monolayer through electrostatic forces and did not displace $PW_{12}O_{40}^{3-}$ from the 3-APTES monolayer on the electrode surface. However, the deposition of PAMAM slightly shifted the $PW_{12}O_{40}^{3-}$ peak potentials, probably because of the strong electrostatic interaction between PAMAM and $PW_{12}O_{40}^{3-}$. This interaction was reported to cause a split of the first anodic peak of $PM_{12}O_{40}^{3-}$ [27].

In order to vary the amount of PtNP-PAMAM deposited on the electrode surfaces, PtNP-PAMAM solutions with differing concentrations were used for electrostatic assembly. This approach was based on the report by Takada et al. [34] in which PAMAM adsorption on electrode surfaces was characterized by an equilibrium relationship between the bulk concentration and the surface coverage. The process was represented by an adsorption isotherm in which short immersion times or very dilute dendrimer solutions resulted in lower surface coverage [35]. In the present study, the quantity of PtNP-PAMAM deposited was estimated from the hydrogen desorption charge from the Pt surface [36].

Figure 3 shows the cyclic voltammetry of PtNP-PAMAM deposited on a monolayer of 3-APTES from different concentrations of the PtNP-PAMAM solution. As seen from the characteristic hydrogen adsorption and desorption peaks in the range, 0.0 to −0.2 V, the amount of PtNPs on the electrode increased when the concentration of the Pt-PAMAM solution used for the assembly step changed from 0.01 mM to 0.2 mM. The quantity of PtNP on the electrode was estimated from these voltammograms. Assuming that the oxidation of one monolayer of H_{ads} on Pt surface corresponds to a charge of 210 μC cm^{-2} [36], the electroactive area for PtNPs encapsulated within PAMAM prepared from 0.2 mM PtNP-PAMAM was estimated as 0.14 cm^2 (curve a, Fig. 3). From the estimated particle size of the PtNPs, 1.4 nm [21], the surface area for one Pt nanoparticle is 6.2×10^{-14} cm^2. Assuming that all the surface of PtNPs in PAMAM was accessible to hydrogen, about 2.3×10^{12} units of PtNP-PAMAM were deposited on the electrode surface, which is equivalent to 3.8×10^{-12} mol cm^{-2} of PtNP-PAMAM. From the molecular diameter of G4-OH PAMAM (4.5 nm), a fully covered surface by PAMAM will contain 5.0×10^{12} units cm^2 (8.2×10^{-12} mol cm^{-2}). Therefore, the estimated surface coverage of PtNP-PAMAM was 46%. Assuming that each PAMAM unit contained 40 Pt atoms (see the Experimental section), the estimated mass of PtNPs on the electrode surface was 30 ng cm^{-2}.

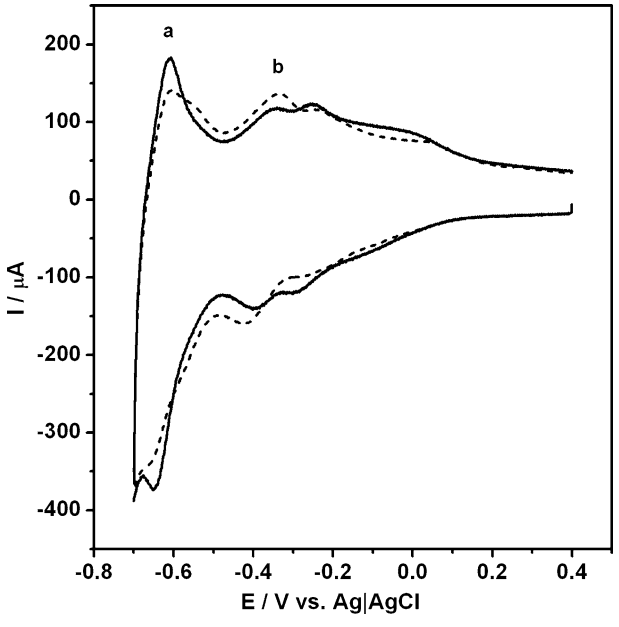

Fig. 2 Effect of PAMAM deposition on the cyclic voltammetry in 0.5 M H_2SO_4 of an ITO|3-APTES|$PW_{12}O_{40}^{3-}$ electrode, **a** before PAMAM deposition, and **b** after PAMAM deposition. The concentration of PAMAM (in 0.1 M H_2SO_4) was 4 μM. Scan rate, 1.0 V s^{-1}

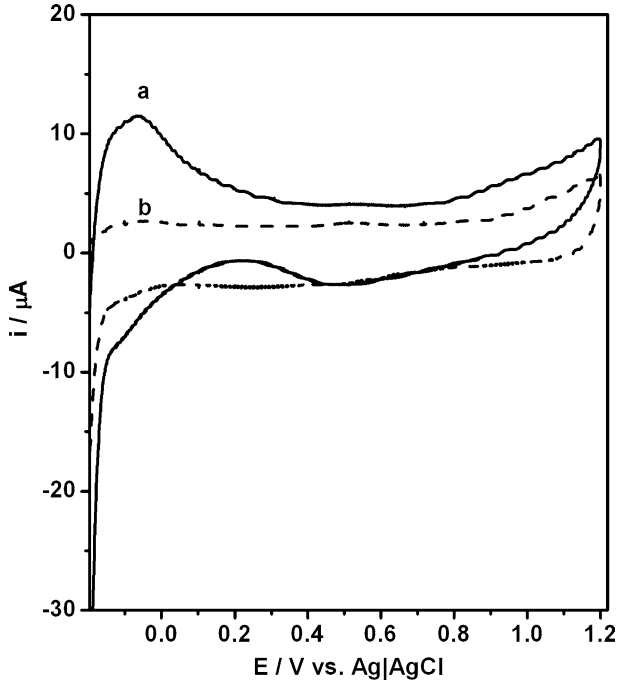

Fig. 3 Cyclic voltammetry of ITO|3-APTES|PtNP-PAMAM electrodes prepared by using **a** 0.2 mM and **b** 0.01 mM PtNP-PAMAM in 0.1 M H_2SO_4. Scan rate, 50 mV s^{-1}; electrolyte, 0.5 M H_2SO_4

The electrocatalytic activity of the ITO|3-APTEs|$PW_{12}O_{40}^{3-}$|PtNP-PAMAM electrodes was tested with the HER (HER). Figure 4 shows the cyclic voltammetry in 0.5 M H_2SO_4 of the electrodes modified with PtNP-PAMAM in the presence and absence of the $PW_{12}O_{40}^{3-}$ monolayer. Here, 0.2 mM PtNP-PAMAM solution was used in the fabrication. The potential range was restricted to the range, 0.4 to −0.7 V, to avoid possible platinum electrodeposition that can result from anodic corrosion of the platinum counter electrode [12]. At the sensitivity used in recording Fig. 4, only the current from the HER was observed. The electrode modified with PtNP-free PAMAM on the $PW_{12}O_{40}^{3-}$ monolayer did not show significant HER before −0.7 V (curve a), whereas the HER on the PtNP-PAMAM modified electrode occurs starting from less than −0.2 V (curve b), consistent with the results on Pt electrodes [37]. This result suggested that the surfaces of encapsulated PtNPs were accessible to hydrogen ions, in agreement with the results reported by Zhao and Crooks [21].

The most significant result in Fig. 4 was that with both PtNP-PAMAM and $PW_{12}O_{40}^{3-}$ present (curve c). In this case, the electrocatalytic activity was significantly greater than that with either component alone. To quantitatively compare the electrocatalytic activities of these electrodes, the current densities of the HER were measured at the starting potential, −0.197 V, and at a mid-potential, −0.4 V (Table 1). With electrodes assembled from a 0.2 mM PtNP-PAMAM solution, the current densities for the initial scans on ITO|3-APTES|$PW_{12}O_{40}^{3-}$|PtNP-PAMAM at these potentials were,

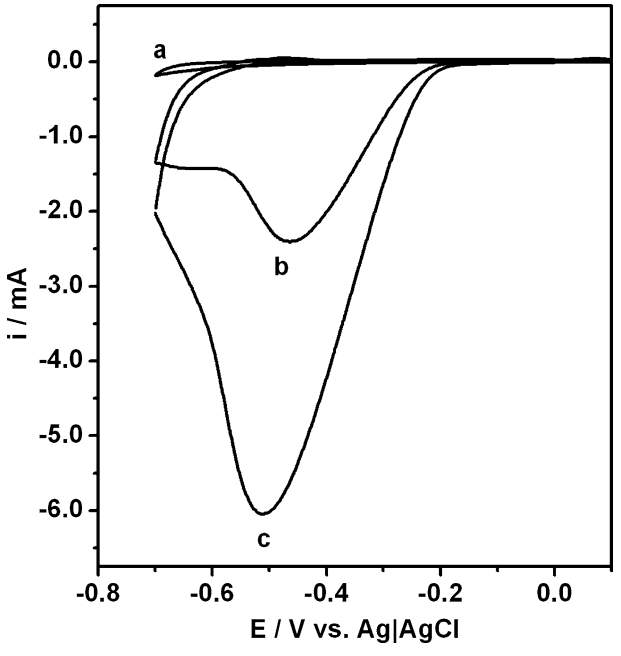

Fig. 4 Cyclic voltammetry of **a** ITO|3-APTES|$PW_{12}O_{40}^{3-}$|PAMAM, **b** ITO|3-APTES|PtNP-PAMAM, and **c** ITO|3-APTES|$PW_{12}O_{40}^{3-}$|PtNP-PAMAM electrodes. The PtNP-PAMAM was deposited from 0.2 mM PtNP-PAMAM in 0.1 M H_2SO_4. Scan rate, 100 mV s^{-1}; initial potential, 0.1 V; electrolyte, 0.5 M H_2SO_4

Table 1 Comparison of the electrocatalytic activities toward the HER on ITO electrodes modified with nanocomposites of PtNP-PAMAM and $PW_{12}O_{40}^{3-}$

Nanocomposite[a]	Current density[b] at −0.197 V (μA cm^{-2})	Current density[b] at −0.4 V (mA cm^{-2})
$PW_{12}O_{40}^{3-}$|PAMAM	−1	−0.02
PtNP-0.2[c]	−40	−2.0
$PW_{12}O_{40}^{3-}$|PtNP-0.2[c]	−110	−4.3
$PW_{12}O_{40}^{3-}$|PtNP-0.05[c]	−110	−5.3
$PW_{12}O_{40}^{3-}$|PtNP-0.02[c]	−4	−0.06
$PW_{12}O_{40}^{3-}$|PtNP-0.01[c]		
Not heated	−1	−0.02
Heated[d]	−20	−2.7

[a]All nanocomposites were deposited on ITO electrode surfaces modified with a 3-APTES monolayer
[b]All current densities were obtained from cyclic voltammetry at 100 mV s^{-1} in 0.5 M H_2SO_4
[c]PtNP-χ refers to PtNP-PAMAM prepared from solutions where χ is the mM concentration of the PtNP-PAMAM solution used in the LBL assembly
[d]The modified electrode was heated at 200 °C for 2 h

respectively, −110 μA cm^{-2} and −4.3 mA cm^{-2}. With a given electrode, the peak currents gradually decreased with scan number; after 10 scans the currents dropped to ca. 50% of the initial values. However, activity was restored by a potential excursion to 1.0 V. The long term stability will be the subject of a future study.

The currents in Fig. 4 were significantly larger than the analogous current densities observed on ITO|3-APTES modified with either PtNP-PAMAM or $PW_{12}O_{40}^{3-}$ alone (Table 1). A similar order of the electrocatalytic activities of the HER was also observed on glassy carbon as the substrate modified with PtNP-PAMAM and $PW_{12}O_{40}^{3-}$ layers, suggesting that the base electrode material had no effect on the electrocatalytic activities of PtNP-PAMAM. Therefore, it can be suggested that there is synergism in the electrocatalytic activity of PtNP-PAMAM and $PW_{12}O_{40}^{3-}$ monolayers.

The ratio of PtNP-PAMAM to $PW_{12}O_{40}^{3-}$ on the ITO|3-APTEs|$PW_{12}O_{40}^{3-}$|PtNP-PAMAM electrode had a significant effect on the electrocatalytic activity toward the HER. The former was deposited from 0.02, 0.05, and 0.2 mM PtNP-PAMAM solutions as described in the Experimental section The electrode prepared from the intermediate concentration, 0.05 mM, showed the highest electrocatalytic activity of this set (Fig. 5). Of particular importance was that the current density observed at −0.4 V (−5.3 mA cm^{-2}) with the electrode prepared from the 0.05 mM solution was larger than the analogous value obtained at the electrode prepared from the 0.2 mM solution (−4.3 mA cm^{-2}). Hence, a larger PtNP density did not result in an increased catalytic efficiency.

The behavior summarized in Table 1 and Fig. 5 is consistent with synergism between PtNPs and $PW_{12}O_{40}^{3-}$ in the catalysis of the HER. An analysis of the factor(s)

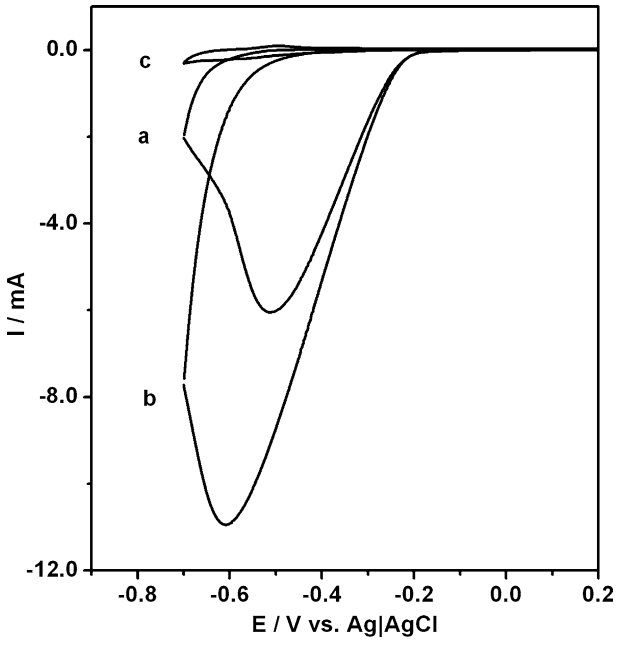

Fig. 5 Cyclic voltammetry of ITO|3-APTES|$PW_{12}O_{40}^{3-}$ |PtNP-PAMAM electrodes prepared from **a** 0.2 mM, **b** 0.05 mM, and **c** 0.02 mM PtNP-PAMAM (in 0.1 M H_2SO_4). Scan rate, 100 mV s^{-1}; electrolyte, 0.5 M H_2SO_4

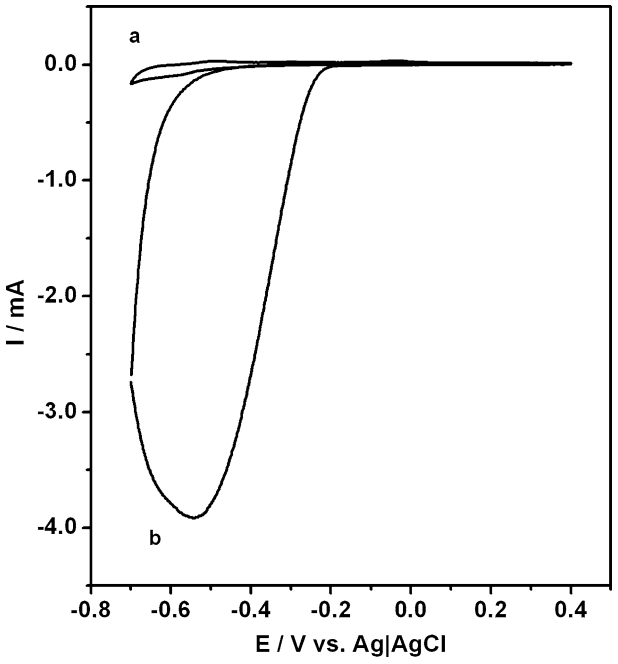

Fig. 6 Cyclic voltammetry of an ITO|3-APTES|$PW_{12}O_{40}^{3-}$ |PtNP-PAMAM electrode prepared from 0.01 mM PtNP-PAMAM before (**a**) and after (**b**) heating at 200 °C for 2 h. Scan rate, 100 mV s^{-1}; electrolyte, 0.5 M H_2SO_4

responsible for this synergism is beyond the scope of this study. However, it is probably related to the "hydrogen spillover" effect that was described for Pt microcenters in $PW_{12}O_{40}^{3-}$ [38, 39] and H_xWO_3 films on Pt surfaces [39]. With the polyoxometalate,

$$PW_{12}O_{40}^{3-} + ne^- + nH^+ \rightleftarrows H_nPW_n^{V}W_{12-n}^{VI}O_{40}^{3-} \quad (1)$$

$$xPt + H_nPW_n^{V}W_{12-n}^{VI}O_{40}^{3-} \rightleftarrows xPtH + H_{n-x}PW_{n-x}^{V}W_{12-n+x}^{VI}O_{40}^{3-} \quad (2)$$

$$2PtH \rightleftarrows 2Pt + H_2 \quad (3)$$

Reaction 2 includes diffusion of proton between the partially reduced polyoxometalate and Pt centers.

Direct contact between the centers was not required for enhancement of the H_2 production by Reactions 1, 2 and 3 [39]. However, given the proposed role of diffusion, decreasing the distance between centers was expected to increase the rate of the HER. To test this supposition, the HER was examined at ITO|3-APTEs|$PW_{12}O_{40}^{3-}$ |PtNP-PAMAM before and after heating the electrode at 200 °C for 2 h in air. With an electrode prepared from 0.01 mM PtNP-PAMAM, the voltammetric current related to the HER was low prior to thermal decomposition of the PAMAM (Fig. 6); with this preparation, only a small amount of PtNP-PAMAM was present on the electrode surface. However, after heated at 200 °C, this modified electrode promoted the HER at a significant level (Fig. 6). Indeed, from the current density, -2.7 mA cm^{-2}, observed at -0.4 V (Table 1), the HER at this electrode was even higher than that on the electrode modified with 0.2 mM PtNP-PAMAM (but not thermally treated), which contained a correspondingly larger amount of PtNPs. The increased electrocatalytic activity of the electrode after heating was attributed to the shorter distance between Pt and $PW_{12}O_{40}^{3-}$ centers, thereby promoting PtH formation (Reaction 2).

Conclusions

Using the LBL electrostatic assembly technique, ordered nanocomposites were assembled on electrode surfaces by depositing PtNP-PAMAM on a monolayer of $PW_{12}O_{40}^{3-}$ that was first deposited on an 3-APTES monolayer. Voltammetric results showed that although the PtNPs were encapsulated within the voids of a PAMAM dendrimer, the surface of the PtNPs was accessible to hydrogen ions; therefore, this modified electrode promoted the HER. Although $PW_{12}O_{40}^{3-}$ may not have direct contact with the PtNPs that were encapsulated within PAMAM dendrimers, the presence of the $PW_{12}O_{40}^{3-}$ monolayer enhanced the electrocatalytic activities of PtNP-PAMAM. Through controlling the quantity of PtNP-PAMAM deposited on the $PW_{12}O_{40}^{3-}$ monolayer, this enhancement was found to depend on the composition of the deposit on the electrodes. These results suggested that there was an interaction that led to a synergistic effect between PtNPs and $PW_{12}O_{40}^{3-}$ in terms of promoting the HER. This effect was significantly increased by heating the composite at 200 °C,

indicating an enhanced interaction between PtNPs and $PW_{12}O_{40}^{3-}$.

Acknowledgements This work was supported in part by the National Science Foundation through grant ECS-0304297.

References

1. Templeton AC, Wuelfing WP, Murray RW (2000) Acc Chem Res 33:27
2. Daniel M, Astruc D (2004) Chem Rev 104:293
3. Wieckowski A, Savinova ER, Vayanas CG (2003) Catalysis and electrocatalysis at nanoparticle surfaces. Marcel Dekker, New York
4. Kulesza PJ, Chojak M, Karnicka K, Miecznikowski K, Palys B, Lewera A (2004) Chem Mater 16:4128
5. Geniès L, Faure R, Durand R (1998) Electrochim Acta 44:1317
6. Maillard F, Martin M, Gloaguen F, Léger JM (1998) Electrochim Acta 47:3431
7. Gloaguen F, Léger JM (1997) J Appl Electrochem 27:1052
8. Ca DV, Sun L, Cox JA (2005) Electrochim Acta (in press)
9. Kao W, Kuwana T (1984) J Am Chem Soc 106:473
10. Savadogo O, Essalik A (1996) J Electrochem Soc 143:1814
11. Savadogo O, Beck P (1996) J Electrochem Soc 143:3842
12. Kulesza PJ, Lu W, Faulkner LR (1992) J Electroanal Chem 336:35
13. Nakajima H, Honma I (2004) Electrochem Solid State Lett 7:A135
14. Savadogo O, Ndzebet E (2001) Int J Hydrogen Energy 26:213
15. Sadakane M, Steckhan E (1998) Chem Rev 98:219
16. Chojak M, Mascetti M, Wlodarczyk R, Marassi R, Karnicka K, Miecznikowski K, Kulesza PJ (2004) J Solid State Electrochem 8:854
17. Tze W, Borzenko MI, Tsirlina GA, Petrii OA (2002) Russ J Electrochem 38:1250
18. Sarathy KV, Raina G, Yadav RT, Kulkarni GU, Rao CNR (1997) J Phys Chem B 101:9876
19. Martel D, Kuhn A, Kulesza PJ, Galkowski MT, Malik MA (2001) Electrochim Acta 46:4197
20. Gloaguen F, Léger JM, Lamy C, Marmann A, Stimming U, Vogel R (1999) Electrochim Acta 44:1805
21. Zhao M, Crooks RM (1999) Adv Mater 11:217
22. Zhao M, Crooks RM (1999) Angew Chem Int Ed 38:364
23. Zhao M, Sun L, Crooks RM (1998) J Am Chem Soc 120:4877
24. Balogh L, Tomalia DA (1998) J Am Chem Soc 120:7355
25. Ye H, Scott RWJ, Crooks RM (2004) Langmuir 20:2915
26. Crooks RM, Zhao M, Sun L, Checkik V, Yeung LK (2001) Acc Chem Res 34:181
27. Cheng L, Cox JA (2001) Electrochem Commun 3:285
28. Kijak AM, Perdue RK, Cox JA (2004) J Solid State Electrochem 8:376
29. He J, Valluzzi R, Yang K, Dolukhanyan T, Song C, Kumar J, Tripathy SK, Samuelson L, Balogh L, Tomalia DA (1999) Chem Mater 11:3268
30. Tokuhisa H, Zhao M, Baker LA, Phan VT, Dermody DL, Garcia ME, Peez RF, Crooks RM, Mayer TM (1998) J Am Chem Soc 120:4492
31. Sun L, Crooks RM (2002) Langmuir 18:8231
32. Kuhn A, Anson FC (1996) Langmuir 12:5481
33. Doron A, Katz E, Willner I (1995) Langmuir 11:1313
34. Takada K, Díaz DJ, Abruña HD, Cuadrado I, Casado C, Alonso B, Morán M, Losada J (1997) J Am Chem Soc 119:10763
35. Hierlemann A, Campbell JK, Baker LA, Crooks RM, Ricco AJ (1998) J Am Chem Soc 120:5323
36. Gloaguen F, Leger JM, Lamy C (1999) J Electroanal Chem 467:186
37. Markovic MM, Grgur BN, Ross PN (1997) J Phys Chem B 101:5405
38. Kulesza PJ, Karwowska B, Grzybowska B, Wieckowski A (1998) Electrochim. Acta 44:1295
39. Timofeeva EV, Tsirlina GA, Petrii OA (2003) Russ J Electrochem 39:716